NIH Public Access
Author Manuscript
Biomater Sci. Author manuscript; available in PMC 2015 October 01.

Published in final edited form as:
Biomater Sci. 2014 October 1; 2(10): 1384–1398. doi:10.1039/C4BM00073K.

Angiopoietin-1 peptide QHREDGS promotes osteoblast differentiation, bone matrix deposition and mineralization on biomedical materials†

Nicole Feric[a], **Calvin C.H. Cheng**[b], **M. Cynthia Goh**[b,c], **Vyacheslav Dudnyk**[d], **Val Di Tizio**[e], and **Milica Radisic**[*,a,e]

[a] Institute of Biomaterials and Biomedical Engineering, University of Toronto, Toronto, Ontario, M5S 3G9 Canada

[b] Department of Chemistry, University of Toronto, Toronto, Ontario M5S 3H6, Canada

[c] Institute for Optical Sciences, University of Toronto, Toronto, Ontario M5S 1A7, Canada

[d] Covalon Technologies Ltd., Mississauga, Ontario L4Z 3E6, Canada

[e] Department of Chemical Engineering and Applied Chemistry, University of Toronto, Toronto, Ontario M5S 3E5, Canada

Abstract

Bone loss occurs as a consequence of a variety of diseases as well as from traumatic injuries, and often requires therapeutic intervention. Strategies for repairing and replacing damaged and/or lost bone tissue include the use of biomaterials and medical implant devices with and without osteoinductive coatings. The soluble growth factor angiopoietin-1 (Ang-1) has been found to promote cell adhesion and survival in a range of cell types including cardiac myocytes, endothelial cells and fibroblasts through an integrin-dependent mechanism. Furthermore, the short sequence QHREDGS has been identified as the integrin-binding sequence of Ang-1 and as a synthetic peptide has been found to possess similar integrin-dependent effects as Ang-1 in the aforementioned cell types. Integrins have been implicated in osteoblast differentiation and bone mineralization, processes critical to bone regeneration. By binding integrins on the osteoblast surface, QHREDGS could promote cell survival and adhesion, as well as conceivably osteoblast differentiation and bone mineralization. Here we immobilized QHREDGS onto polyacrylate (PA)-coated titanium (Ti) plates and polyethylene glycol (PEG) hydrogels. The osteoblast differentiation marker, alkaline phosphatase, peaked in activity 4-12 days earlier on the QHREDGS-immobilized PA-coated Ti plates than on the unimmobilized, DGQESHR (scrambled)- and RGDS-immobilized surfaces. Significantly more bone matrix was deposited on the QHREDGS-immobilized Ti surface than on the other surfaces as determined by atomic force microscopy. The QHREDGS-immobilized hydrogels also had a significantly higher mineral-to-matrix (M/M) ratio determined by Fourier transform infrared spectroscopy. Alizarin Red S and von Kossa staining and quantification, and environmental scanning electron microscopy showed that while both the QHREDGS- and RGDS-immobilized surfaces had extensive mineralization

†Electronic supplementary informa on (ESI) available. See DOI:

*m.radisic@utoronto.ca; Tel.: +1 416 946 5295; Fax: +1 416 978 4317.

NIH-PA Author Manuscript
NIH-PA Author Manuscript
NIH-PA Author Manuscript

NIH-PA Author Manuscript

NIH-PA Author Manuscript

NIH-PA Author Manuscript

relative to the unimmobilized and DGQESHR-immobilized surfaces, the mineralization was more considerable on the QHREDGS-immobilized surface, both with and without the induction of osteoblast differentiation. Finally, treatment of cell monolayers with soluble QHREDGS was demonstrated to upregulate osteogenic gene expression. Taken together, these results demonstrate that the QHREDGS peptide is osteoinductive, inducing osteoblast differentiation, bone matrix deposition and mineralization.

1. INTRODUCTION

Bone loss can result from a traumatic injury or from a variety of diseases including infection, osteoporosis, arthritis, or cancer [1]. While biomaterials and medical implant devices are used to restore, maintain, and/or improve the function of lost or damaged bone [2, 3], the gold standard for treatment is still autologous bone grafts despite decades of ongoing research [4]. Yet, autologous bone is a less than ideal material because it is both limited in its availability and bone harvesting can induce donor site morbidity [5, 6]. These issues have been addressed to a degree by the development of allogeneic cadaveric bone tissue, but this material is itself associated with a number of challenges including infection and/or host immune response [7, 8]. Meanwhile, research into biomaterials and medical implant devices has advanced these technologies from simple structural supports to materials that actively promote bone regeneration [1, 3], but while they can promote osteoblast attachment, migration and growth, few can stimulate osteoblast differentiation and bone mineralization, i.e. promote bone formation [3].

Interactions between the extracellular matrix (ECM) and integrin-type receptors initiate important signaling pathways for osteogenic differentiation and bone formation [9]. Hence research is underway to investigate the potential of targeting integrins as a means of increasing bone formation and repair [9]. Integrins are heterodimeric transmembrane adhesion receptors composed of α- and β-subunits that mediate the transduction of signals [10] and have been identified as important for all stages of bone generation: osteoblast adhesion and differentiation ($\alpha_1\beta_1$, $\alpha_2\beta_1$, $\alpha_4\beta_1$, $\alpha_5\beta_1$, $\alpha_{11}\beta_1$, and $\alpha_v\beta_3$); osteoblast survival ($\alpha_2\beta_1$, $\alpha_{11}\beta_1$); bone mineralization (α_5, β_1, $\alpha_v\beta_3$ and $\alpha_2\beta_1$); and *in vivo* bone formation ($\alpha_4\beta_1$, $\alpha_5\beta_1$) [9,11]. The integrin ligand angiopoietin-1 (Ang-1)—a 498 amino acid, multi-domain secreted glycoprotein [12]—has been identified to effectively promote cell adhesion and survival in a variety of cell types, including fibroblasts, skeletal myocytes and cardiac myocytes [13, 14], thus exhibiting features that suggest it has potential as a regulator of bone formation and repair. However, the size and complexity of Ang-1 limit its ability to function in the context of medical device coatings and biomaterials but opportunely, the eponymous 7 amino acid peptide QHREDGS—the integrin-binding site of Ang-1 [14]—is equally effective as a pro-adhesion, pro-survival molecule in various cell types [15, 16]. Immobilizing entire proteins in medical devices presents challenges related to cost of recombinant growth factor production, as well as the possibility of denaturation during the immobilization procedure or storage. These challenges can be overcome through the use of short, linear peptides. Moreover, the peptide QHREDGS was demonstrated to act through $\alpha_5\beta_1$ and $\alpha_v\beta_3$ receptors in endothelial cells [15]. Given the role of integrins in bone formation—particularly of the β_1 subtype, identified to participate in all stages of bone development—and of the ability of QHREDGS

NIH-PA Author Manuscript

NIH-PA Author Manuscript

NIH-PA Author Manuscript

to interact with these receptors, we sought to determine if QHREDGS could promote bone formation, specifically by inducing osteoblast differentiation and bone mineralization.

Medical devices to treat bone loss are frequently composed of titanium (Ti) due to its advantageous physical properties and biocompatibility [17]. However, Ti can deteriorate upon implantation [18] and the extent of bone formation and repair it can achieve remains below the standards for successful treatment [19]. Coatings have been developed to improve upon the existing attributes. Polyacrylate (PA) coatings prevent corrosion and reduce metal ion release without compromising the biocompatibility [20], while also allowing for covalent immobilization of bioactive molecules that can improve the osteogenic capacity of the Ti device. The development of biomaterials used to treat bone loss have progressed through the identification of new biocompatible materials as well as the identification of bioactive molecule modifiers that induce bone growth [21, 22]. But these too have had limited success because the quantities of growth factors needed to induce bone formation is in vast excess of physiological levels and local application is required to avoid complication such as ectopic bone formation, necessitating very controlled release of these factors [23]. We therefore sought to determine if QHREDGS could be used to improve the success of both medical implant devices and biomaterials to treat bone loss by investigating the effectiveness of the QHREDGS peptide in inducing bone formation while immobilized onto PA-coated Ti medical plates or inert polyethylene glycol (PEG) hydrogels. PA-coated Ti medical plates were used since they are an example of clinically used material, while inert PEG hydrogels were used to isolate the effect of the immobilized peptide on the cells, as PEG hydrogels are inherently non-adhesive and non-fouling.

2. MATERIALS & METHODS

MG-63 human osteosarcoma cells (ATCC, Manassas, VA)

Uncoated and polyacrylate-coated titanium plates (a gift from Covalon Technologies Ltd., Mississauga, ON) Custom peptide DGQESHR (Biomatik Corporation, Cambridge, ON)

Custom peptide RGDS (Biomatik Corporation, Cambridge, ON)

Custom peptide NH_2-QHREDGS-$CONH_2$ (Institute for Biomolecular Design, Edmonton, AB)

Custom Peptide FITC-aminohexanoic acid-QHREDGS-$CONH_2$ (Institute for Biomolecular Design, Edmonton, AB)

Poly(ethylene glycol) diacrylate, M_n 700 (Sigma Aldrich, Oakville, ON)

Acrylate-PEG-NHS Ester MW 3500 (Jenkem Technologies, Allen, TX)

GelBond PAG Film (Lonza, Basel, CH)

22×22mm Vinyl coverslips (Bel-Art Scienceware, Wayne, NJ)

2-Hydroxy-2-methyl-propiophenone (Sigma Aldrich, Oakville, ON)

NIH-PA Author Manuscript

NIH-PA Author Manuscript

NIH-PA Author Manuscript

Dulbecco's Phosphate-Buffered Saline without Ca^{2+}, Mg^{2+} (Gibco/Life Technologies, Burlington, ON)

2.1.Peptide Immobilization to Polyacrylate (PA)-Coated Titanium (Ti) Plates

To quantify the amount of QHREDGS peptide conjugated to the Ti plates (5mm × 5mm × 0.3mm), uncoated or PA-coated Ti plates were placed in a solution containing the conjugating reagents ethyl(dimethylaminopropyl) carbodiimide (EDC; Thermo Scientific, Rockford, IL) and Sulfo-*N*-hydroxysuccinimide (NHS; Thermo Scientific) in a 1:2.5 molar ratio in ddH_2O for 15min shaking at 700rpm at 20°C. To determine if QHREDGS interacted non-specifically with the PA-coating, PA-coated Ti plates were also incubated with NHS in the absence of EDC. After 15min, the Ti plates were incubated in a solution of 150μg FITC-labeled QHREDGS (FITC-QHREDGS, reconstituted in phosphate buffered saline, PBS) in ddH_2O for 3h shaking at 700rpm at 20°C, then placed to wash in excess ddH_2O overnight at 4°C. The reaction and wash solutions were read in a SpectraMax GeminiXS fluorescent plate reader with SoftMax Pro 3.2.1 software (Molecular Devices, Sunnyvale, CA) and the amount of FITC-QHREDGS therein was determined from a standard curve. The amount of FITC-QHREDGS conjugated to the plate was determined by subtracting the sum of the amounts of peptide in the solutions from the original amount of peptide added. Direct measurement of the Ti plates was not possible because of fluorescence quenching by the non-transparent substrate.

For experiments, uncoated and PA-coated Ti plates were incubated with EDC/NHS as outlined above, then incubated in solutions of PBS with or without 320μM peptide (QHREDGS, RGDS or DGQESHR, reconstituted in PBS) for 3h shaking at 700rpm at 20°C. The plates were washed, as above, then placed into low attachment 24-well culture plates (Corning Inc., Corning, NY) in 70% ethanol overnight under UV in a biosafety cabinet. The sterilized plates were washed twice with sterile PBS and then left to air dry for 5 minutes prior to cell seeding.

2.2.Peptide Immobilization to Polyethylene Glycol (PEG) Hydrogels

To quantify the amount of QHREDGS peptide conjugated to the PEG hydrogels, FITC-QHREDGS peptide was incubated with 4.0mg acrylate-PEG-NHS in a 100μL solution of 50mM Tris pH 8.5 containing 0μL, 10μL, 20μL, or 40μL of 50mM FITC-QHREDGS solution (reconstituted in PBS) for 3h shaking at 700rpm at 20°C. After 3h, the reaction solutions were diluted to 1mL with ddH_2O and dialyzed extensively against ddH_2O. The dialyzed reaction solutions were lyophilized and resuspended in 80μL ddH_2O. The amount of FITC-QHREDGS contained in the reconstituted solution was determined from a standard curve using a SpectraMax GeminiXS fluorescent plate reader and SoftMax Pro 3.2.1 software.

For experiments, the peptides were incubated with 4.0mg acrylate-PEG-NHS in a 100μL solution of 50mM Tris pH 8.5 with or without 10μL of 50mM peptide (QHREDGS, RGDS or DGQESHR, reconstituted in PBS) for 3h shaking at 700rpm at 20°C. After 3 h, the reaction solutions were diluted with ddH_2O to 1mL and dialyzed extensively against ddH_2O. The dialyzed reaction solutions were lyophilized and resuspended in ddH_2O, to which

NIH-PA Author Manuscript

NIH-PA Author Manuscript

NIH-PA Author Manuscript

polyethylene glycol diacrylate (PEGDA) was added in a ratio of 50mol PEGDA to 1mol acrylate-PEG-NHS, containing 0.5% w/w 2-hydroxy-2-methyl-propiophenone in a final volume of 80μL. For each hydrogel, 25μL of this solution was pipetted onto a 22×22mm square of GelBond PAG film and a vinyl coverslip of equal size was gently placed on top. The hydrogel was placed under a UV light for 10mins to polymerize, then placed into low attachment 6-well culture plate (Corning Inc., Corning, NY) washed in PBS for 10min on a shaker and then incubated at 4°C for 1h. After 1 h, the coverslip was gently peeled off the hydrogel with tweezers and the hydrogel was placed in 70% ethanol under UV light for 1 h to sterilize. Sterilized hydrogels were incubated in DMEM/10%FBS medium overnight prior to seeding with cells.

2.3.Cell Culture

MG-63 human osteosarcoma cells were grown to confluence in T-25 flasks in DMEM (Gibco) with 10% FBS (Gibco) and 10% Penstrep (Gibco). All experiments were performed on cell passages 5-8. To seed the Ti plates, the cells were washed with PBS, dissociated with 0.05% trypsin (Gibco), centrifuged for 5min at 2000rpm and resuspended in a minimum volume of culture medium. The cells were counted and 3-5μL of cell suspension was pipetted onto the centre of the 25mm^2 Ti plate at a density of 3200 cells per 25mm^2 plate (day 0). The seeded plates were then incubated at 37°C for 30min to permit the cells to adhere, at which point 1mL of media was added to each well gently. As controls, media was added to wells in the absence of Ti plates with or without an equal volume of cell suspension. The conditioned media was collected from the wells every other day and replaced with fresh media. Beginning day 12, the media was supplemented with 50μg/mL α-ascorbic acid, 10mM β-glycerophosphate and 100nM dexamethasone (osteogenic media) and cultured for a total of 34 days. The conditioned media samples were aliquoted and stored at -20°C until needed. Additionally, Ti plates were seeded with 200,000 cells per 25mm^2 plate and cultured for 22 days in DMEM/10% FBS media without any supplementation (non-osteogenic media).

The PEG hydrogels were seeded as described above, but with some modifications. The cells were counted and 100μL of cell suspension was pipetted onto the centre of the 484mm^2 hydrogel at a density of 62,000 cells (day 0) such that the seeding cell density was the same for the Ti plates and PEG hydrogels. After incubation at 37°C for 30min, 4mL of media was added to each well gently. Beginning day 15, the hydrogels were switched to the osteogenic media and cultured for a total of 41 days. On day 41, cells bound to the hydrogel were determined by washing with PBS, dissociating with 0.05% trypsin (Gibco), centrifuging for 5min at 2000rpm, resuspending the cells and performing 6 separate counts per hydrogel using a hemocytometer.

For dose response experiments, MG-63 cells were seeded into 24-well polystyrene tissue culture plates in DMEM with 10% FBS in the presence of 5, 50 or 500μM soluble QHREDGS or equivolume PBS (1% volume). Once cells were confluent, media was supplemented with 50μg/mL α-ascorbic acid, 10mM β-glycerophosphate and 100nM dexamethasone (osteogenic media) and cells were cultured for an additional 22 days. Over

NIH-PA Author Manuscript

NIH-PA Author Manuscript

NIH-PA Author Manuscript

the course of the culture period, the media was changed every other day and additional QHREDGS/PBS was added with each media change.

2.4.Alizarin Red S and von Kossa Staining

The seeded Ti plates were fixed on day 22 or 34 in 4% paraformaldehyde (PFA) for 15min at 20°C. The plates were washed once with ddH_2O and then incubated with a stain solution of 1% Alizarin Red S (Sigma Aldrich) in ddH_2O for 5min at 20°C. Plates were washed twice with ddH_2O and then imaged using an Olympus CKX41 inverted microscope at 10× magnification, with an Olympus SC30 Digital Camera and Olympus cellSense Digital Imaging Software (Olympus America Inc., Center Valley, PA). Following Alizarin Red S staining and imaging, the plates were subjected to von Kossa staining. The plates were washed thrice in ddH_2O; incubated with a stain solution of 5% silver nitrate in ddH_2O for 30min; washed thrice; developed with a freshly made solution of 5% sodium carbonate in 2.5% formaldehyde in ddH_2O for 5min; washed thrice; fixed with a solution of 5% sodium thiodisulphate for 2min; washed thrice; and then re-imaged.

To quantify the amount of Alizarin Red S bound to the various surfaces, images were analyzed using ImageJ software (NIH, Bathesda, MD). The images were first split into red, green and blue channels, and the red channel images were used for all further analysis. For the Ti plates cultured in osteogenic medium, the mineralization was too extensive on some surfaces to distinguish mineral deposits, therefore the raw integrated density (sum of pixel values) of the images was measured. For the Ti plates cultured in non-osteogenic medium and the hydrogels, the red channel images were thresholded and the percent area of staining was measured.

2.5.Alkaline Phosphatase Activity Assay

The alkaline phosphatase (ALP) activity of the conditioned medium samples collected from the seeded Ti plates was measured using Alkaline Phosphatase Yellow Liquid p-nitrophenol phosphate (pNPP) substrate for ELISA (Sigma Aldrich) as previously described [24] with some modification. Briefly, all samples and the pNPP substrate were allowed to come to room temperature before beginning the assay, then 10μL of sample was added to wells of a 96-well plate, to which 100μL of the pNPP substrate was added. Immediately after addition of the substrate, the plate was read at 405nm every 10 seconds for 30min in a Molecular Devices VersaMax Tunable microplate reader (Molecular Devices, Sunnyvale, CA). The ALP activity (IU/L) was calculated from the formula:

$$\frac{(OD_{\mathrm{t}} - OD_0) \times 1000 \times total \quad volume}{t \times 18.75 \quad mM^{-1}cm^{-1} \times path \quad length \times sample \quad volume}$$

2.6.Glucose Consumption Assay

The glucose content of the conditioned medium samples collected from the seeded Ti plates was measured using a QuantiChrom Glucose Assay Kit (BioAssay Systems, Hayward, CA), performed according to supplier instructions.

NIH-PA Author Manuscript

NIH-PA Author Manuscript

NIH-PA Author Manuscript

2.7.Cytotoxicity Assay

The lactate dehydrogenase (LDH) content of the conditioned medium samples collected from the seeded Ti plates was measured using a LDH Cytotoxicity Assay Kit (Cayman Chemical Company, Ann Arbor, MI), performed according to supplier instructions.

2.8.Quantitative PCR

MG-63 monolayers were grown in 24-well polystyrene tissue culture plastic in the presence of 5, 50 or 500μM soluble QHREDGS or equivolume PBS in osteogenic media for 22 days. RNA was isolated every four days, reverse transcribed into cDNA and qPCR was performed, as previously described[25], using primers for bone sialoprotein, osteocalcin, collagen type I and β-actin as previously described[26] and alkaline phosphatase, as previously described[27]. Expression levels were normalized to the housekeeping gene β-actin.

2.9.Attenuated Total Reflectance (*ATR*) Fourier Transform Infrared (*FTIR*) spectroscopy

On day 41, seeded hydrogels were fixed in 4% PFA, washed with ddH_2O, and then analyzed by ATR-FTIR spectroscopy. On day 34, seeded Ti plates were fixed in 4% PFA, washed extensively over a period of weeks with ddH_2O to remove the mineral and then analyzed by ATR-FTIR spectroscopy. Transmission spectra were obtained using an ATR top-plate accessory coupled to a Spectrum One FTIR spectrometer with a fast recovery deuterated triglycine sulfate detector (PerkinElmer, Inc., Waltham, MA). The spectra were recorded in the region between 4000 and 650 cm^{-1}. For each Ti plate or hydrogel, 5-11 randomly selected regions were measured and for each spectrum, at least 4 scans were averaged. The peak areas were determined from baseline-corrected absorbance spectra using SPECTRUM software (PerkinElmer). The collagen (matrix) concentration of the bone matrix was determined by combining the areas of the absorbance peaks in the regions of 1720 (amide I), 1640 (amide II) and 1250 cm^{-1} (amide III). The phosphate (mineral) content of the bone matrix was determined from the areas of the absorbance peaks in the region of 900-1200 cm^{-1}. The ratio of mineral-to-matrix (M/M ratio) was determined by dividing the phosphate concentration by the collagen concentration.

2.10. Atomic Force Microscopy (AFM)

Titanium plates seeded with 3200 cells per $25mm^2$ plate, cultured in osteogenic medium for a total of 34 days and fixed in 4% PFA. The plates were washed extensively over a period of weeks with ddH_2O to remove the mineral and then subjected to contact mode AFM. Force spectroscopy measurements, yielding force-distance curves, were performed in ddH_2O using a JPK NanoWizard II AFM (JPK Instruments AG, Berlin, Germany). Measurements were conducted at ambient temperature and the samples were conscientiously maintained in a hydrated state. The cantilevers used were V-shaped silicon nitride cantilevers with a spring constant of 0.1 N/m (Bruker, Camarillo, CA). The cantilever deflection sensitivity was obtained by indenting the tip against a glass substrate and the tip radius was measured to be 26nm. Three to six sections of the surface were measured and a 10μm × 10μm area was scanned per section, with probe velocities of 1-5μm/s. To determine the Young's modulus, a Hertzian model was applied to the extension force-displacement curves with the appropriate fit range manually determined for each curve using JPK Image Processing Software (JPK

NIH-PA Author Manuscript

NIH-PA Author Manuscript

NIH-PA Author Manuscript

Instruments AG, Berlin, Germany). In our calculations, we assumed the tip to be a paraboloidal indenter.

2.11. Environmental Scanning Electron Microscopy (SEM)

The Ti plates seeded at a density of 200,000 cells per 25mm^2 and cultured for 22 days in non-osteogenic media, were fixed for 30min in 4% PFA/1% glutaraldehyde, washed with ddH_2O and imaged using a Hitachi VP-SEM S3400N Variable Pressure SEM (Hitachi High Technologies America, Inc., Roslyn Heights, NY) at low vacuum (70Pa) with an accelerating voltage of 15kV. Images were taken with two magnifications using the backscatter (BSE) detector.

2.12. Statistical Analysis

Analyses of two groups were made with Student's *t* test. Analyses of more than two groups were performed using a one-way ANOVA with Student's–Newman–Keuls (SNK) multiple-comparison test for normally distributed data and a Kruskal-Wallis one-way ANOVA on ranks with Dunn's post-hoc analysis for data that failed the normality test using SigmaPlot 12 software (Systat Software Inc, San Jose, CA) with $P < 0.05$ considered to be significant.

3. RESULTS

3.1.QHREDGS peptide can be immobilized on polyacrylate (PA)-coated titanium (Ti) and polyethylene glycol (PEG)-based hydrogels using ethyl(dimethylaminopropyl) carbodiimide (EDC)- and N-hydroxysulfosuccinimide (NHS)-based chemistry

Initial experiments were performed to demonstrate that the small peptide QHREDGS could be immobilized onto PA-coated Ti plates and PEG hydrogels using basic EDC/NHS-based immobilization chemistry. Since the functionality of the peptide is not orientation-dependent, a specific conjugation method was not required and EDC/NHS chemistry was chosen for its frequent usage in such applications. We quantified the amount of peptide that was immobilized by using a FITC-labeled variant (FITC-QHREDGS). Peptides do not readily react with titanium unless the surface has been modified to facilitate covalent immobilization; herein titanium plates were coated with polyacrylate, which has reactive carboxylic groups to which peptides can be conjugated. Both the uncoated Ti plates incubated with the fluorescently-labeled peptide in the presence of both NHS and EDC and the PA-coated Ti plates incubated with NHS in the absence of EDC had a detectable amount of FITC-QHREDGS associated with them (14.7±6.1μg and 16.3±6.7μg of FITC-QHREDGS, respectively; **Fig.1A**); however the amount of FITC-QHREDGS associated with the plates under these conditions did not differ significantly ($P > 0.05$, n=3; **Fig.1A**). Thus, the peptide can physically absorb equally well onto both uncoated and PA-coated Ti, indicating that coating Ti with polyacrylate does not promote non-specific, non-covalent binding. In the presence of EDC, an additional 18.7±5.2μg of FITC-QHREDGS was specifically and covalently immobilized to the PA-coated Ti plate resulting in an immobilized peptide surface concentration of 0.33±0.09μg/mm^2 (0.27±0.08nmol/mm^2), a significant increase in the amount of peptide relative to either the uncoated Ti ($P = 0.02$, n=3; **Fig.1A**) or the PA-coated Ti plate in the absence of EDC ($P = 0.03$, n=3; **Fig.1A**). The efficiency of the FITC-QHREDGS immobilization to PA-coated Ti was 15.61±3.0% (**Fig.**

NIH-PA Author Manuscript

NIH-PA Author Manuscript

NIH-PA Author Manuscript

1B), which was significantly higher than for the uncoated Ti plate ($P = 0.005$, n=3; **Fig.1B**) or the PA-coated Ti plate in the absence of EDC ($P = 0.02$, n=3; **Fig.1B**).

Similarly, FITC-QHREDGS was conjugated to PEG hydrogels by incubating the peptide with a bifunctional PEG derivative, acrylate-PEG-NHS, which was then incorporated into the hydrogel. Increasing the concentration of FITC-QHREDGS incubated with the acrylate-PEG-NHS resulted in an increased amount of FITC-QHREDGS bound to the PEG derivative producing hydrogels with FITC-QHREDGS concentrations of 4.1±1.6mg/mL (3.4±1.3nM) for the 6mg/mL reaction solution, 7.9±1.7mg/mL (6.5±1.4nM) for the 12mg/mL solution and 11.7±4.5mg/mL (9.7±3.7nM) for the 24mg/mL solution (**Fig.1C**). The immobilization efficiency ranged from 34-75% for the 6mg/mL FITC-QHREDGS reaction solution, 41-63% for the 12mg/mL solution, and 24-53% for the 24mg/mL solution (**Fig.1D**). Increasing the reaction solution concentration from 6mg/mL to 12mg/mL resulted in a significant increase in the amount of FITC-QHREDGS that was immobilized to the PEG derivative ($P = 0.003$, n=3; **Fig.1C**), but did not significantly improve the efficiency ($P > 0.05$, n=3; **Fig.1D**). Increasing the reaction solution concentration from 12mg/mL to 24mg/mL did not significantly increase the amount of immobilized FITCQHREDGS ($P > 0.05$, n=3; **Fig.1C**) but significantly reduced the immobilization efficiency ($P = 0.04$, n=3; **Fig.1D**).

3.2.QHREDGS immobilization to PA-coated Ti accelerates osteoblast differentiation

Alkaline phosphatase (ALP), a marker of osteoblast differentiation, is a cell surface enzyme located on the outer plasma membrane of osteoblasts [28] where it catalyzes the hydrolysis of phosphomonoesters (R-O-PO_3) releasing inorganic phosphate [29]; a process that promotes bone mineralization. MG-63 osteoblast-like cells were grown to confluence on Ti plates with variable coatings (with and without peptides) and induced to differentiate on day 12 by culturing the cells in osteogenic medium. On day 18, the ALP activity detected in the conditioned media did not differ significantly between the various treatment groups (**Fig.2**). By day 22, the amount of ALP activity detected in the conditioned media of the cells grown on PA-coated Ti plates with immobilized QHREDGS was significantly more than detected in the conditioned media of the cells grown on any other surfaces ($P < 0.05$; n = 3; **Fig.2**). The amount of ALP activity detected in the conditioned media of MG-63 cells grown on polystyrene tissue culture plastic or on uncoated Ti did not change significantly over the course of the assay ($P > 0.05$, n=3; **Fig.2**). Conversely, the amount of ALP activity detected in the conditioned media of cells grown on any of the various PA-coated Ti surfaces did significantly increase with maxima on day 22 for the QHREDGS-immobilized surface, on day 26 for the RGDS-immobilized and on day 34 for both the PA-Coated Ti plate (without any peptide) and DGQESHR-immobilized surfaces (**Fig.2**); however, the ALP activity maxima did not vary significantly ($P > 0.05$, n=3). The amount of ALP activity detected in the conditioned medium of cells grown on the DGQESHR-immobilized surface on day 34 was found to be inconsistent with wide ranging values, however it did not differ significantly from the negligible amount of activity detected from the conditioned medium of cells grown on the low-attachment polystyrene surface (0.25±0.12IU/L and 0.0079±0.0079IU/L, respectively; $P > 0.05$, n=3; **Fig.2**).

NIH-PA Author Manuscript

NIH-PA Author Manuscript

NIH-PA Author Manuscript

The significant increase in ALP activity on day 22 in the conditioned media of cells grown on the QHREDGS-immobilized surface cannot be attributable to increased metabolic activity as there was no significant difference in glucose consumption at this time point for the QHREDGS-immobilized surface relative to any other surface ($P > 0.05$, n=3; **Fig.S1**). While there was a 40% increase on average in glucose consumption between day 18 and day 22 for the cells grown on the QHREDGS-immobilized surface, the increase was non-significant and these glucose consumption values did not differ significantly from those measured for the other surfaces ($P > 0.05$, n=3; **Fig.S1**). Similarly, the amount of cell death —as determined by the lactate dehydrogenase (LDH) activity in the conditioned medium— decreased 40% on average between day 18 and day 22 for the QHREDGS-immobilized surfaces, however this decrease was not significant, nor did the LDH activities on either day 18 or day 22 differ significantly from that measured for the other surfaces (**Fig.S2**). The amount of cell death did not change significantly over the culture period for any of the peptide-immobilized surfaces ($P > 0.05$; n =3; **Fig.S2**) and the amount of cell death on the QHREDGS-immobilized surface did not differ significantly from the other surfaces ($P > 0.05$; n = 3; **Fig.S2**). Neither glucose consumption (**Fig.S1**) nor LDH activity (**Fig.S2**) varied significantly between the surfaces over the duration of the culture period, indicating that the surface modifications did not adversely or advantageously affect cellular metabolic activity or cell death.

3.3.Soluble QHREDGS promotes upregulation of osteogenic genes

In order to determine the effect of treatment with soluble QHREDGS peptide, MG-63 cells were grown to confluence on tissue culture plastic and treated with soluble peptide for a 22-day period of culture in osteogenic medium. At various time points, the cells were lysed, RNA was extracted and qPCR was performed to determine the effect of increasing QHREDGS peptide concentration on the gene expression of ALP, osteocalcin, collagen type I and bone sialoprotein. Relative to the control equivolume PBS treatment, a concentration of 5μM QHREDGS added to the media resulted in a notable increase in ALP gene expression on day 10; and a QHREDGS concentration of 50μM resulted in increased ALP gene expression on days 6-14 relative to the control (**Fig.3A** and **Fig.S3A**). Interestingly, treatment with 500μM QHREDGS did not increase ALP gene expression relative to the control. Osteocalcin gene expression was significantly upregulated by 50μM treatment on day 6 ($P = 0.05$, n=3; **Fig.3B** and **Fig.S3B**) but was significantly downregulated by 500μM QHREDGS treatment on day 14 ($P = 0.03$, n=3; **Fig.3B** and **Fig.S3B**) relative to the control. Collagen type I gene expression was also significantly upregulated on day 10 with 5μM QHREDGS treatment ($P = 0.05$, n=3; **Fig.3C** and **Fig.S3C**) and on day 14 by 50μM QHREDGS ($P = 0.002$, n=3; **Fig.3C** and **Fig.S3C**), and significantly downregulated by 500μM QHREDGS treatment on day 22 ($P = 0.01$, n=3; **Fig.3C** and **Fig.S3C**), relative to the control. Finally, bone sialoprotein gene expression was significantly increased on day 6 and 10 with 5μM QHREDGS treatment ($P = 0.03$, $P = 0.04$, respectively, n=3; **Fig.3D** and **Fig.S3D**) and on day 14 by 50μM QHREDGS ($P = 0.05$, n=3; **Fig.3D** and **Fig.S3D**), whereas 500μM QHREDGS treatment did not have a significant effect on expression.

NIH-PA Author Manuscript

NIH-PA Author Manuscript

NIH-PA Author Manuscript

3.4.QHREDGS immobilization to PA-coated Ti promotes collagen production

Bone is a connective tissue that is predominantly comprised of an extracellular matrix (ECM) consisting of collagen, non-collagenous proteins, minerals (primarily hydroxyapatite) and water [30, 31]. The bone ECM produced by the MG-63 osteoblast-like cells grown on the variously-coated Ti plates was assessed by Fourier transform infrared (FTIR) spectroscopy and by atomic force microscopy (AFM). The surface composition of the demineralized bone was determined by FTIR. The surface collagen concentration of the bone matrix produced on the QHREDGS-immobilized PA-coated Ti plates was significantly higher than that produced by cells grown on the uncoated Ti plates ($P < 0.05$, n = 4; **Fig. 4A**), but not statistically different from that of the other PA-coated Ti plates ($P > 0.05$, n = 4; **Fig.4A**). The total amount of demineralized ECM produced by the cells grown on the various Ti plates was determined by calculating the elastic (Young's) moduli of the demineralized bone surfaces by AFM, with a smaller elastic modulus indicating the presence of more demineralized ECM. The average elastic modulus of the QHREDGS-immobilized PA-coated Ti surface was lower than for all other surfaces investigated, and significantly lower than all surfaces excepting the uncoated and DGQESHR (scrambled)-immobilized PA-coated Ti surface ($P < 0.05$; n ≥ 9; **Fig.4B**). Notably, the bottom 8% of elastic modulus values were derived exclusively from measurements of regions on QHREDGS-immobilized plates, values that account for approximately one-third of the total QHREDGS-immobilized plate measurements (**Fig.4B**).

3.5.QHREDGS immobilization to PA-coated Ti and to PEG hydrogels promotes bone mineralization

Successful bone formation is evaluated by matrix mineralization. Mineralization can be assessed by calcium and phosphate staining, Alizarin Red S and von Kossa dyes respectively, and by environmental scanning electron microscopy (ESEM) with a BSE detector, wherein calcium-based minerals appear as bright spots against the surrounding ECM due to the higher atomic number. For seeded Ti plates cultured in osteogenic medium and grown for a total of 34 days, we observed little to no staining on the uncoated Ti surface (**Fig.5A**) and a patchy staining pattern on the PA-coated Ti without any peptide immobilized (**Fig.5B**). Conversely, the QHREDGS-immobilized plate (**Fig.5C**) staining was consistent throughout and more extensive than on either the RGDS-immobilized plate (**Fig.5D**), wherein the staining was spotty amid larger areas of consistent staining, and the DGQESHR (scrambled)-immobilized PA-coated Ti (**Fig.5E**) surface that showed a very patchy pattern of staining. Quantification of the amount of Alizarin Red S stain bound to the surfaces indicated a significant increase in the amount of staining on the QHREDGS-immobilized surface relative to the uncoated, PA-coated Ti without any peptide immobilized and the DGQESHR (scrambled)-immobilized Ti surfaces ($P < 0.05$; n = 3; **Fig.6**); as well as increased staining relative to the RGDS-immobilized surface (**Fig.6**). Notably, seeded Ti plates cultured in nonosteogenic medium and grown for 22 days also showed the same pattern of Alizarin Red S and von Kossa staining, albeit mineralization was less extensive on all surfaces (**Fig.S4**). Quantification of the amount of Alizarin Red S stain bound to the Ti surfaces, again showed that staining was increased on the QHREDGS-immobilized Ti relative to all other surfaces (**Fig. S5**). By ESEM imaging, no evidence of mineralization

NIH-PA Author Manuscript

NIH-PA Author Manuscript

NIH-PA Author Manuscript

(bright spots) was seen on the uncoated Ti plate surface (**Fig.S6A-B**). However, on the QHREDGS-immobilized PA-coated Ti plate mineralization was evident as relatively large regions (**Fig.S6C-D**) that were decidedly more numerable than on the RGDS-immobilized surface wherein mineralization was visible as small granules with larger localized regions (**Fig.S6E-F**).

The staining of PEG hydrogels with or without peptides immobilized showed an analogous pattern to the Ti plates for Alizarin Red S and von Kossa staining. Specifically, minimal staining was evident on the PEG hydrogel without peptide (**Fig.S7A**), while staining on the QHREDGS-immobilized hydrogels (**Fig.S7B**) appeared more extensive than on either the RGDS- (**Fig.S7C**) or DGQESHR (scrambled)-immobilized hydrogels (**Fig.S7D**). On both the RGDS- and QHREDGS-immobilized hydrogels staining was punctate, but the stained regions on the QHREDGS-immobilized hydrogel appeared to be more closely clustered relative to the RGDS-immobilized hydrogel. Quantification of the amount of Alizarin Red S bound to the surfaces showed that the QHREDGS-immobilized surface had significantly more stain bound than either the hydrogel without any peptide immobilized or the DGQESHR (scrambled)-immobilized hydrogel surface ($P < 0.05$; n = 3; **Fig.S8**), whereas a similar amount of stain bound as the RGDS-immobilized surface (**Fig.S8**).

The surface composition of the bone ECM on the various PEG hydrogels was determined by FTIR and quantification of the extent of bone mineralization was achieved by calculating the mineral-to-matrix ratio (M/M ratio) [32-35]. The surface collagen (matrix) concentration of the bone ECM generated by the cells on the hydrogels was found to be lower on average for the QHREDGS-immobilized hydrogel relative to all other hydrogels but not significantly different ($P > 0.05$; n=4; **Fig.7A**). Conversely, the phosphate (mineral) concentration on the hydrogel surface was higher on average for the QHREDGS-immobilized hydrogel than for any other hydrogel surface but once again this difference was not statistically different ($P > 0.05$; n=4; **Fig.7B**). However the M/M ratio of the QHREDGS-immobilized hydrogel was significantly increased relative to all other surfaces ($P < 0.05$; n=4; **Fig.7C**). The significant increase in bone mineralization was not a consequence of increased cell number because while the number of cells on the QHREDGS-immobilized hydrogel was more than on both the PEG hydrogel without any peptide immobilized and the DGQESHR-immobilized hydrogel, it was less than on the RGDS-immobilized hydrogel ($P > 0.05$; n=4; **Fig.S6**), and yet bone mineralization was more extensive for the QHREDGS-immobilized hydrogel than any other surface.

4. DISCUSSION

Using standard treatment techniques, there still remains a substantial fraction of bone defects that do not heal properly [7]. Small animal models have demonstrated the promise of gene therapy and stem/progenitor cell transplantation, however major safety and efficacy concerns need to be addressed before their clinical application [36, 37]. Thus, much effort has been directed alternatively in designing biomaterials for the controlled delivery of osteoinductive factors in order to produce a highly localized tissue response [4]. Herein we have demonstrated that the small Ang-1-derived peptide QHREDGS can be covalently immobilized to both PA-coated Ti and PEG hydrogels through EDC/NHS-based chemistry

NIH-PA Author Manuscript

NIH-PA Author Manuscript

NIH-PA Author Manuscript

(**Fig.1**), thereby localizing the effect of the peptide to the surface of the medical device/ biomaterial. The use of QHREDGS in bone therapy applications is advantageous in that its conjugation is amenable to different biomedical materials, which we demonstrated by covalently immobilizing QHREDGS to two very different surface types using the ubiquitous chemistry of EDC/NHS. Additionally, since the functionality of the QHREDGS peptide is not dependent upon any particular conformation or orientation, there is flexibility in the conjugation methods that can be used for immobilization, further expanding the variety of contexts in which QHREDGS can be used. Interestingly, the effective concentration of QHREDGS seems to be relatively low since high concentrations (500μM) were observed to downregulate the osteogenic genes collagen type I and osteocalcin (**Fig.3** and **S3**). Finally, as a small 7-amino acid peptide, QHREDGS can be easily and cost-effectively synthesized, and can withstand a higher degree of manipulation and a wider range of conditions than a full-length protein.

Moreover, we have demonstrated that QHREDGS is osteoinductive, promoting osteoblast differentiation along with both bone matrix deposition and mineralization. Osteoblast differentiation is oftentimes marked by ALP activity, an enzyme secreted in increasing amounts during the second phase of osteoblast differentiation, matrix deposition [39], with levels peaking before the cells transition into the third stage of differentiation, matrix mineralization [40]. The ALP activity of osteoblast-like cells cultured on QHREDGS-immobilized Ti plates peaked 4-12 days earlier than on the unimmobilized, DGQESHR (scrambled)- or RGDS-immobilized surfaces, with all the surfaces ultimately achieving the same maximum ALP activity (**Fig.2**). This is indicative of an accelerated rate of osteoblast differentiation on the QHREDGS-immobilized surface but not of increased differentiation overall. Similarly, we also observed that treatment of osteoblasts with soluble QHREDGS induced the upregulation of osteogenic genes (**Fig.3** and **Fig.S3**). The time required for bone regeneration is a critical factor for successful bone therapy; furthermore decreased healing time reduces a patient's recovery time, i.e. their discomfort, stress and economic costs, but also reduces the risk of complications [41]. Hence, by accelerating the rate of osteoblast differentiation, QHREDGS may also improve bone regeneration success.

Much like ALP activity, bone composition can be used to make assumptions about the formation of bone. Bone strength is determined by both bone quantity and quality [42]; and among the factors that dictate bone quality are *toughness*, the domain of the collagen fibers tasked with providing the properties of ductility and energy absorption as well as *stiffness*, determined by the mineral phase [43]. Osteoblast-like cells cultured on the QHREDGS-immobilized Ti produced a bone matrix that when demineralized did not differ significantly in the relative surface composition among the various PA-coated Ti surfaces (**Fig.4A**) but had a significantly lower elastic modulus than produced on the other surfaces (**Fig.4B**), indicating that QHREDGS-immobilization produced quantitatively more bone matrix compared to the other surfaces. The elastic modulus of demineralized bone is positively correlated with bone strength, work-to-fracture and toughness [44], however in this context the significant reduction in local elastic modulus denotes a change from the stiff Ti surface to a surface coated with extracellular matrix proteins. Importantly, this change in elastic modulus describes a change in localized mechanical properties, whereas if a bulk test of mechanical

NIH-PA Author Manuscript

NIH-PA Author Manuscript

NIH-PA Author Manuscript

properties were to be performed, the elastic modulus would still be governed by the Ti plate itself. Currently, Ti-based scaffolds are being designed with elastic moduli approximating that of bone [45], a value that varies from 4 to 30 GPa depending on the type of bone measured and the measurement direction [46]. This is because a biomechanical mismatch wherein the implant has a higher stiffness than bone can result in “stress shielding”—the inhibition of stress transfer to the adjacent bone—that can result in bone resorption around the implant and ultimately implant loosening and failure [47]. In order to take advantage of the mechanical strength of the device while at the same time permitting the effective communication of the cells with their surroundings, it is thought that the ideal implant would precisely combine high strength with a low modulus closer to the bone [48]. As such, based on our findings, QHREDGS-immobilization can generate a low elastic modulus environment on the implant surface that promotes osteoblast differentiation and bone production without affecting the overall strength of the device, and thereby has the potential to reduce the risk of implant failure.

The relative surface composition of the mineralized bone matrix produced on the QHREDGS-immobilized PEG hydrogels was measured to be lower in collagen content than the other hydrogel surfaces (**Fig.7A**). While seemingly contradictory, an inverse relationship between collagen content and the degree of mineralization has been reported [49], and in fact we observed that the QHREDGS-immobilized hydrogel surface also had more mineral content than the other hydrogel surfaces as this inverse relationship would predict (**Fig.7B**). Moreover, it is quite likely that the collagen content on the QHREDGS-immobilized surface was measured to be lower because the matrix was covered by a mineral layer and FTIR is a technique that measures surface composition, as IR light penetration is on the order of micrometers during ATR measurements. Given the high mineral and low collagen (matrix) measurements for the QHREDGS-immobilized surface, it is unsurprising that the resultant mineral-to-matrix (M/M) ratio was significantly higher for the QHREDGS-immobilized surface than the other surfaces (**Fig.7C**). The M/M ratio by definition indicates the relative amount of mineral and matrix, and is used as a measure of bone mineralization [32]. Notably, there is a positive correlation between the M/M ratio and total bone mineral density, load to failure and bone stiffness [42]. Thus, QHREDGS-immobilization induces bone mineralization to a greater degree than the other surfaces. This fact was also evident in our imaging data wherein both the QHREDGS- and RGDS-immobilized surfaces had extensive mineral staining that was quantified to be increased on the QHREDGS-immobilized Ti surface, both when osteoblasts were induced to differentiate (**Fig.5-6**) and when they were not (**Fig.S4-5**); and quantified to be equivalent on the PEG-immobilized surfaces (**Fig.S7-8**). Taken together, these results demonstrate that QHREDGS-immobilization induces matrix deposition and its subsequent mineralization, and suggests that QHREDGS can induce the production of better quality bone.

While QHREDGS is a relatively new bioactive molecule, and an entirely novel factor for bone regenerative therapy, the RGD peptide has long been investigated within the context of both titanium [50-52] and hydrogels [53, 54]. Herein we have demonstrated the improved effectiveness of QHREDGS over RGDS with respect to osteoblast differentiation, bone matrix deposition and mineralization. This indicates both the potential for improved

NIH-PA Author Manuscript

NIH-PA Author Manuscript

NIH-PA Author Manuscript

therapeutic results with the QHREDGS peptide over the RGD peptide, and for pushing forward research into this novel factor by substitution of one peptide for the other in existing therapies given the similarities between RGD and QHREDGS. Although, it is unlikely that QHREDGS will improve bone regeneration success rates to the needed levels on its own, its improved osteoinductive properties can provide an incremental step forward. As new medical devices/biomaterials and approaches are developed the QHREDGS peptide can be used to supplement these new technologies with minimal necessary adjustments given its manipulability and flexibility.

In terms of a possible mechanism, QHREDGS has been reported to bind to β_1-type integrins with specific interactions noted between the peptide and $\alpha_5\beta_1$ and $\alpha_v\beta_3$ integrin receptors [15] ; and β_1-integrins have been identified as playing a significant role in osteoblast differentiation, mineralization *in vitro* and bone formation *in vivo* [9, 11]. Herein, we demonstrate that the QHREDGS peptide affects the *in vitro* processes of matrix deposition and mineralization, and osteoblast differentiation. This may suggest that QHREDGS affects these processes through a β_1-integrin-mediated pathway. Recently, knockdown of the β_1-integrin binding partner integrin-linked kinase (ILK) was shown to result in increased differentiation and bone mineralization by downregulating c-JUN-dependent transcription [55]. Conversely, activation of extracellular signal-related kinase ($ERK_{1/2}$) pathway downstream of ILK has been reported to promote differentiation and bone mineralization [56, 57]. The precise molecular mechanisms involved in improved bone mineralization by QHREDGS is therefore unclear and will be the subject of future work.

5. CONCLUSIONS

We have demonstrated for the first time that the small Ang-1-derived peptide QHREDGS accelerates osteoblast differentiation and promotes both bone matrix deposition and mineralization more effectively than the common integrin-binding peptide RGDS, when immobilized to either titanium medical devices or biomaterials. The acceleration of the processes of osteoblast differentiation, matrix deposition and bone mineralization are important factors influencing bone therapy as the time needed to regenerate bone affects not only the ultimate success of the treatment but can also affects the recovery time for the patient. Additionally, the ability of QHREDGS-immobilization to modify the localized mechanical properties of implant devices without affecting its global mechanical properties has the potential to reduce the risk of implant failure. Finally, we have demonstrated that the quality of the bone produced by the QHREDGS-immobilized surfaces was improved relative to the other surfaces investigated. Hence, the novel peptide QHREDGS may be a suitable candidate for tests in preclinical models.

Supplementary Material

Refer to Web version on PubMed Central for supplementary material.

Acknowledgments

To Michael Sefton, a great leader, visionary and a truly outstanding mentor.

NIH-PA Author Manuscript

NIH-PA Author Manuscript

NIH-PA Author Manuscript

This work was funded by grants from Natural Sciences and Engineering Research Council of Canada (NSERC) Strategic Grant (STPGP 381002-09), Ontario Research Fund–Global Leadership Round 2 (ORF-GL2), Canadian Institutes of Health Research (CIHR) Operating Grant (MOP-126027), NSERC-CIHR Collaborative Health Research Grant (CHRPJ 385981-10), NSERC Discovery Grant (RGPIN 326982-10), NSERC Discovery Accelerator Supplement (RGPAS 396125-10), National Institutes of Health Grant (2R01 HL076485) and Heart and Stroke Foundation Grant (T6946). Electron microscopy was performed at the University of Toronto, Faculty of Medicine, Microscopy Imaging Lab with the help of Battista Calvieri. FTIR was performed at the University of Toronto, Analytical Lab for Environmental Science Research and Training (ANALEST) facility. The graphical abstract was designed by Boyang Zhang.

ABBREVIATIONS

Ang-1	angiopoietin-1
PA	polyacrylate
Ti	titanium
PEG	polyethylene glycol
M/M	mineral-to-matrix
EDC	ethyl(dimethylaminopropyl) carbodiimide
NHS	sulfo-*N-hydroxysuccinimide*
ALP	alkaline phosphatase
LDH	lactate dehydrogenase
ECM	extracellular matrix
FTIR	Fourier transform infrared spectroscopy
AFM	atomic force microscopy
ESEM	environmental scanning electron microscopy
ILK	integrin-linked kinase
$ERK_{1/2}$	extracellular signal-related kinase

References

1. Miron RJ, Zhang YF. J. Dent. Res. 2012 (DOI:10.1177/0022034511435260).
2. Anderson DG, Burdick JA, Langer R. Science. 2004; 305:1923–1924. (DOI:10.1126/science.1099987). [PubMed: 15448260]
3. Singhatanadgit W. Bone and Tissue Regeneration Insights. 2009; 2:1–11.
4. Lienemann PS, Lutolf MP, Ehrbar M. Adv. Drug Deliv. Rev. 2012; 64:1078–1089. (DOI:10.1016/j.addr.2012.03.010; 10.1016/j.addr.2012.03.010). [PubMed: 22465487]
5. Arrington ED, Smith WJ, Chambers HG, Bucknell AL, Davino NA. Clin. Orthop. Relat. Res. 1996:329, 300–309.
6. Sasso RC, Williams JI, Dimasi N, Meyer PR Jr. J. Bone Joint Surg. Am. 1998; 80:631–635. [PubMed: 9611023]
7. Bishop GB, Einhorn TA. Int. Orthop. 2007; 31:721–727. (DOI:10.1007/s00264-007-0424-8). [PubMed: 17668207]
8. Geiger M, Li RH, Friess W. Adv. Drug Deliv. Rev. 2003; 55:1613–1629. [PubMed: 14623404]
9. Marie PJ. Nat. Rev. Endocrinol. 2013; 9:288–295. (DOI:10.1038/nrendo.2013.4; 10.1038/nrendo.2013.4). [PubMed: 23358353]

NIH-PA Author Manuscript NIH-PA Author Manuscript NIH-PA Author Manuscript

10. Takada Y, Ye X, Simon S. Genome Biol. 2007; 8:215. (DOI:10.1186/gb-2007-8-5-215). [PubMed: 17543136]
11. Schneider GB, Zaharias R, Stanford C. J. Dent. Res. 2001; 80:1540–1544. [PubMed: 11499509]
12. Davis S, Aldrich TH, Jones PF, Acheson A, Compton DL, Jain V, Ryan TE, Bruno J, Radziejewski C, Maisonpierre PC, Yancopoulos GD. Cell. 1996; 87:1161–1169. [PubMed: 8980223]
13. Carlson TR, Feng Y, Maisonpierre PC, Mrksich M, Morla AO. J. Biol. Chem. 2001; 276:26516–26525. (DOI:10.1074/jbc.M100282200). [PubMed: 11346644]
14. Dallabrida SM, Ismail N, Oberle JR, Himes BE, Rupnick MA. Circ. Res. 2005; 96:e8–24. (DOI: 10.1161/01.RES.0000158285.57191.60). [PubMed: 15692086]
15. Miklas JW, Dallabrida SM, Reis LA, Ismail N, Rupnick M, Radisic M. PLoS One. 2013; 8:e72956. (DOI:10.1371/journal.pone.0072956; 10.1371/journal.pone.0072956). [PubMed: 24013716]
16. Rask F, Dallabrida SM, Ismail NS, Amoozgar Z, Yeo Y, Rupnick MA, Radisic M. J. Biomed. Mater. Res. A. 2010; 95:105–117. (DOI:10.1002/jbm.a.32808). [PubMed: 20540095]
17. Mazzola L, Bemporad E, Misiano C, Pepe F, Santini P, Scandurra R. J. Nanosci Nanotechnol. 2011; 11:8754–8762. [PubMed: 22400255]
18. Olmedo DG, Tasat DR, Duffo G, Guglielmotti MB, Cabrini RL. Acta Odontol. Latinoam. 2009; 22:3–9. [PubMed: 19601489]
19. Dimitriou R, Jones E, McGonagle D, Giannoudis PV. BMC Med. 2011:9. 66-7015-9-66 (DOI: 10.1186/1741-7015-9-66; 10.1186/1741-7015-9-66. [PubMed: 21269451]
20. De Giglio E, Cafagna D, Ricci MA, Sabbatini L, Cometa S, Ferretti C, Mattioli-Belmonte M. Journal of Bioactive and Compatible Polymers. 2010; 25:374–391. (DOI: 10.1177/0883911510372290).
21. Li RH, Wozney JM. Trends Biotechnol. 2001; 19:255–265. [PubMed: 11412949]
22. Hollinger JO, Schmitt JM, Buck DC, Shannon R, Joh SP, Zegzula HD, Wozney J. J. Biomed. Mater. Res. 1998; 43:356–364. [PubMed: 9855194]
23. Carragee EJ, Hurwitz EL, Weiner BK. Spine J. 2011; 11:471–491. (DOI:10.1016/j.spinee. 2011.04.023; 10.1016/j.spinee.2011.04.023). [PubMed: 21729796]
24. Ravichandran R, Ng CC, Liao S, Pliszka D, Raghunath M, Ramakrishna S, Chan CK. Biomed. Mater. 2012; 7 015001-6041/7/1/015001. Epub 2011 Dec 9 (DOI:10.1088/1748-6041/7/1/015001; 10.1088/1748-6041/7/1/015001).
25. Nunes SS, Miklas JW, Liu J, Aschar-Sobbi R, Xiao Y, Zhang B, Jiang J, Masse S, Gagliardi M, Hsieh A, Thavandiran N, Laflamme MA, Nanthakumar K, Gross GJ, Backx PH, Keller G, Radisic M. Nat. Methods. 2013; 10:781–787. (DOI:10.1038/nmeth.2524; 10.1038/nmeth.2524). [PubMed: 23793239]
26. Zhang W, Li Z, Peng B. J. Endod. 2010; 36:1978–1982. (DOI:10.1016/j.joen.2010.08.038; 10.1016/j.joen.2010.08.038). [PubMed: 21092816]
27. Kim HK, Kim MG, Leem KH. Food Funct. 2014; 5:573–578. (DOI:10.1039/c3fo60509d; 10.1039/c3fo60509d). [PubMed: 24496382]
28. Harrison G, Shapiro IM, Golub EE. J. Bone Miner. Res. 1995; 10:568–573. (DOI:10.1002/jbmr. 5650100409). [PubMed: 7610927]
29. Holtz KM, Kantrowitz ER. FEBS Lett. 1999; 462:7–11. [PubMed: 10580082]
30. Fujisawa R, Tamura M. Front. Biosci. 2012; 17:1891–1903.
31. Nicolaije C, Koedam M, van Leeuwen JP. J. Cell. Physiol. 2012; 227:1309–1318. (DOI:10.1002/jcp.22841; 10.1002/jcp.22841). [PubMed: 21604266]
32. Paschalis EP, DiCarlo E, Betts F, Sherman P, Mendelsohn R, Boskey AL. Calcif. Tissue Int. 1996; 59:480–487. [PubMed: 8939775]
33. Paschalis EP, Mendelsohn R, Boskey AL. Clin. Orthop. Relat. Res. 2011; 469:2170–2178. (DOI: 10.1007/s11999-010-1751-4; 10.1007/s11999-010-1751-4). [PubMed: 21210314]
34. Takata S, Shibata A, Yonezu H, Yamada T, Takahashi M, Abbaspour A, Yasui N. J. Med. Invest. 2004; 51:133–138. [PubMed: 15460898]
35. Weiss P, Bohic S, Lapkowski M, Daculsi G. J. Biomed. Mater. Res. 1998; 41:167–170. [PubMed: 9641637]

NIH-PA Author Manuscript

NIH-PA Author Manuscript

NIH-PA Author Manuscript

36. Fischer J, Kolk A, Wolfart S, Pautke C, Warnke PH, Plank C, Smeets R. J. Craniomaxillofac. Surg. 2011; 39:54–64. (DOI:10.1016/j.jcms.2010.03.016; 10.1016/j.jcms.2010.03.016). [PubMed: 20434921]
37. Guldberg RE. J. Bone Miner. Res. 2009; 24:1507–1511. (DOI:10.1359/jbmr.090801; 10.1359/jbmr.090801). [PubMed: 19653806]
38. Puklin-Faucher E, Sheetz MP. J. Cell. Sci. 2009; 122:179–186. (DOI:10.1242/jcs.042127; 10.1242/jcs.042127). [PubMed: 19118210]
39. Kulterer B, Friedl G, Jandrositz A, Sanchez-Cabo F, Prokesch A, Paar C, Scheideler M, Windhager R, Preisegger KH, Trajanoski Z. BMC Genomics. 2007; 8:70. (DOI:10.1186/1471-2164-8-70). [PubMed: 17352823]
40. Stein GS, Lian JB, Owen TA. FASEB J. 1990; 4:3111–3123. [PubMed: 2210157]
41. Victoria G, Petrisor B, Drew B, Dick D. Indian. J. Orthop. 2009; 43:117–120. (DOI:10.4103/0019-5413.50844; 10.4103/0019-5413.50844). [PubMed: 19838359]
42. Takata S, Yonezu H, Shibata A, Enishi T, Sato N, Takahashi M, Nakao S, Komatsu K, Yasui N. J. Med. Invest. 2011; 58:197–202. [PubMed: 21921420]
43. Viguet-Carrin S, Garnero P, Delmas PD. Osteoporos. Int. 2006; 17:319–336. (DOI:10.1007/s00198-005-2035-9). [PubMed: 16341622]
44. Wang X, Shen X, Li X, Agrawal CM. Bone. 2002; 31:1–7. [PubMed: 12110404]
45. Li J, Yang H, Wang H, Ruan J. Mater. Sci. Eng. C. Mater. Biol. Appl. 2014; 34:110–114. (DOI:10.1016/j.msec.2013.08.043; 10.1016/j.msec.2013.08.043). [PubMed: 24268239]
46. Katz JL. Nature. 1980; 283:106–107. [PubMed: 7350519]
47. Sumner DR, Turner TM, Igloria R, Urban RM, Galante JO. J. Biomech. 1998; 31:909–917. [PubMed: 9840756]
48. Geetha M, Singh AK, Asokamani R, Gogia AK. Progress in Materials Science. 2009; 54:397–425.
49. Aerssens J, Boonen S, Lowet G, Dequeker J. Endocrinology. 1998; 139:663–670. [PubMed: 9449639]
50. Ferris DM, Moodie GD, Dimond PM, Gioranni CW, Ehrlich MG, Valentini RF. Biomaterials. 1999; 20:2323–2331. [PubMed: 10614938]
51. Schliephake H, Scharnweber D, Dard M, Rossler S, Sewing A, Meyer J, Hoogestraat D. Clin. Oral Implants Res. 2002; 13:312–319. [PubMed: 12010163]
52. Elmengaard B, Bechtold JE, Soballe K. J. Biomed. Mater. Res. A. 2005; 75:249–255. (DOI:10.1002/jbm.a.30301). [PubMed: 16106438]
53. Alsberg E, Anderson KW, Albeiruti A, Franceschi RT, Mooney DJ. J. Dent. Res. 2001; 80:2025–2029. [PubMed: 11759015]
54. Burdick JA, Anseth KS. Biomaterials. 2002; 23:4315–4323. [PubMed: 12219821]
55. El-Hoss J, Arabian A, Dedhar S, St-Arnaud R. Gene. 2014; 533:246–252. (DOI:10.1016/j.gene.2013.09.074; 10.1016/j.gene.2013.09.074). [PubMed: 24095779]
56. Choi YH, Gu YM, Oh JW, Lee KY. Biochem. Biophys. Res. Commun. 2011; 415:472–478. (DOI:10.1016/j.bbrc.2011.10.097; 10.1016/j.bbrc.2011.10.097). [PubMed: 22056560]
57. Wanachewin O, Boonmaleerat K, Pothacharoen P, Reutrakul V, Kongtawelert P. BMC Complement. Altern. Med. 2012:12. 71-6882-12-71 (DOI:10.1186/1472-6882-12-71; 10.1186/1472-6882-12-71). [PubMed: 22380404]

NIH-PA Author Manuscript
NIH-PA Author Manuscript
NIH-PA Author Manuscript

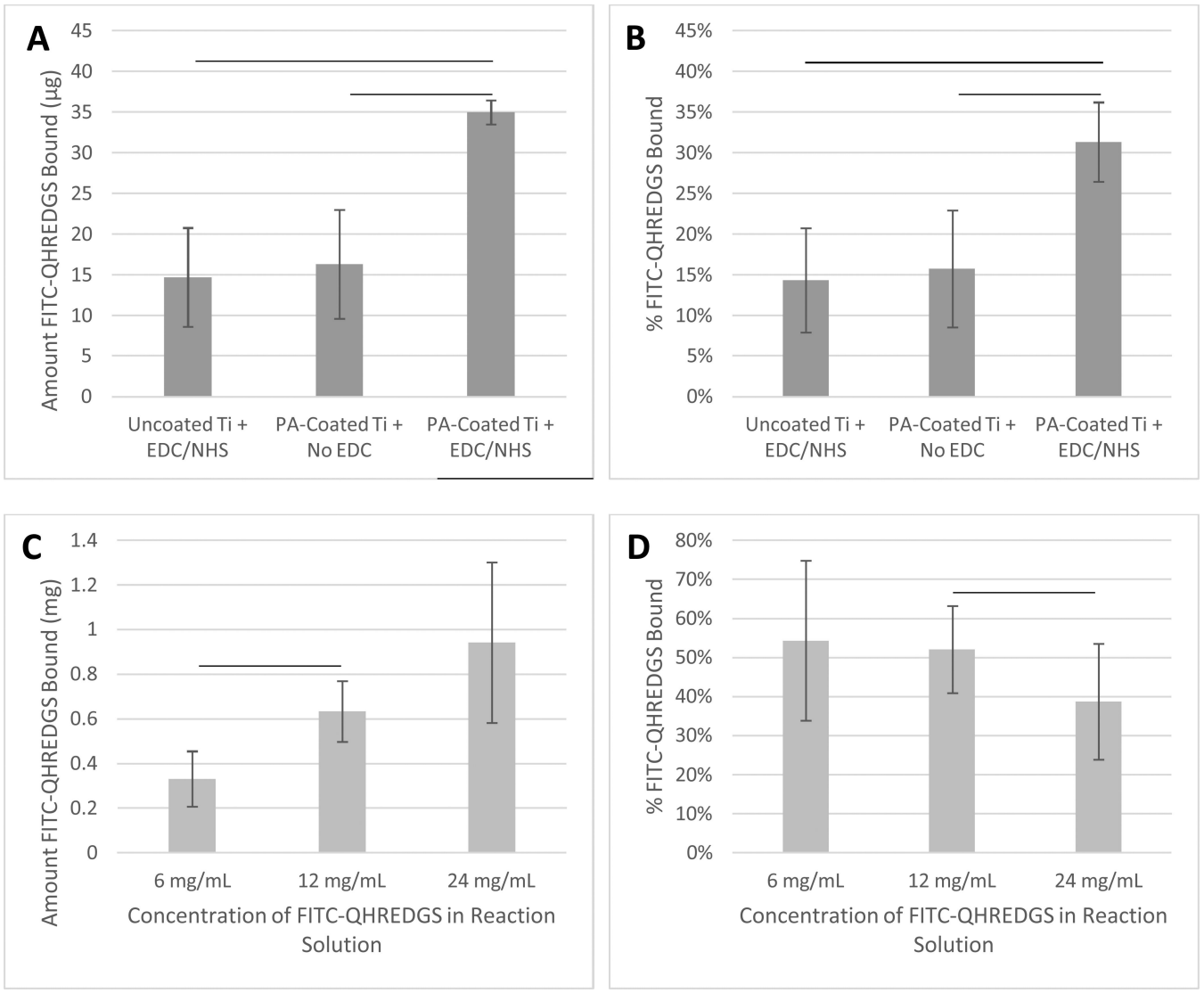

Figure 1.

Covalent immobilization of QHREDGS to PA-coated Ti plates using EDC/NHS chemistry and to PEG hydrogels using acrylate-PEG-NHS. Uncoated or PA-coated Ti plates were placed in a reaction mixture containing FITC-QHREDGS and the conjugating reagent NHS in the presence or absence of EDC: **(A)** the amount of FITCQHREDGS peptide bound to Ti plate; **(B)** the percentage of FITC-QHREDGS bound to the Ti plate of the initial amount added to the reaction solution. The PEG-derivative acrylate-PEG-NHS was incubated in a reaction mixture containing different concentrations of QHREDGS-FITC: **(C)** the amount bound to the PEG-derivative in the hydrogel; **(D)** the percentage of FITC-QHREDGS bound to the PEG-derivative of the initial amount of peptide added to the reaction solution. The data presented are the mean ± the SEM (n=3) and the lines indicate statistical significance ($P < 0.05$; one-way ANOVA and Student-Newman-Keuls post-hoc analysis; n=3).

NIH-PA Author Manuscript

NIH-PA Author Manuscript

NIH-PA Author Manuscript

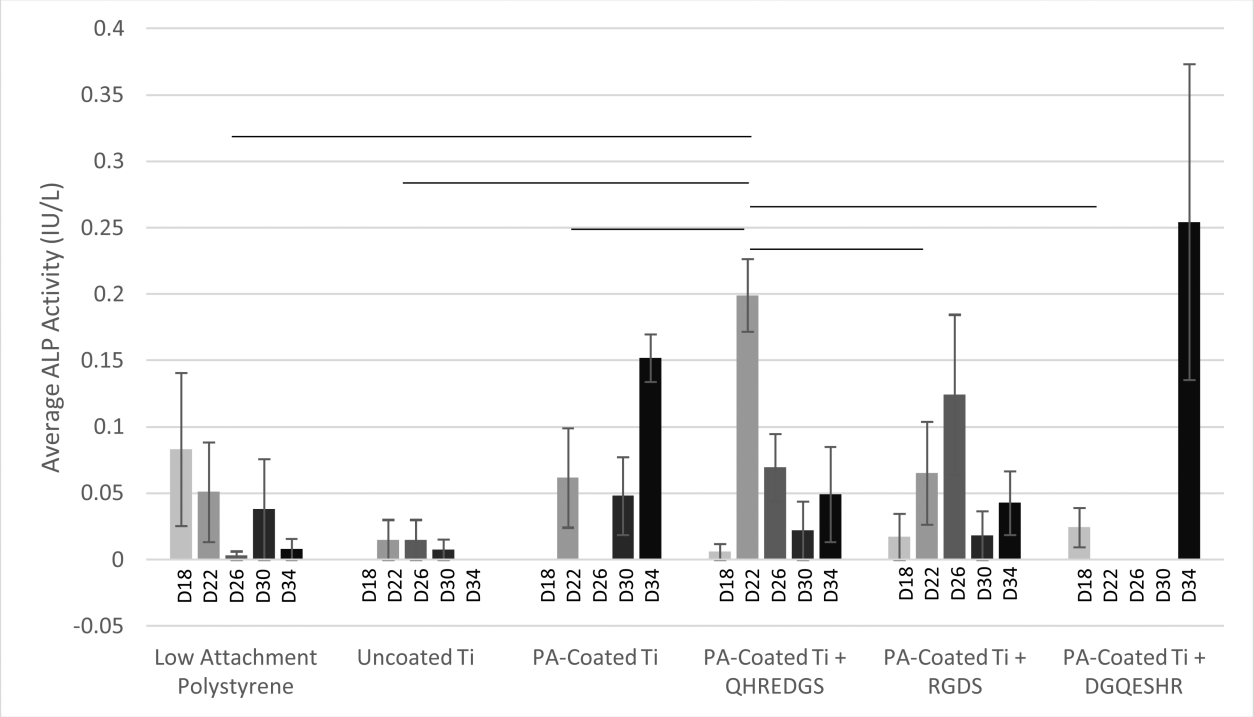

Figure 2.

Alkaline phosphatase (ALP) activity measured in conditioned medium collected on the indicated day (D) of osteoblasts grown on low attachment polystyrene tissue culture plastic or Ti plates without PA-coating (*Uncoated Ti*), with PA-coating but no peptide conjugated (*PA-Coated Ti*), or with PA-coating and either QHREDGS, RGDS or DGQESHR (scrambled) peptide conjugated. Data presented are the mean ± SEM and the lines indicate statistical significance ($P < 0.05$; one-way ANOVA and Student-Newman-Keuls post-hoc analysis; n=3).

NIH-PA Author Manuscript
NIH-PA Author Manuscript
NIH-PA Author Manuscript

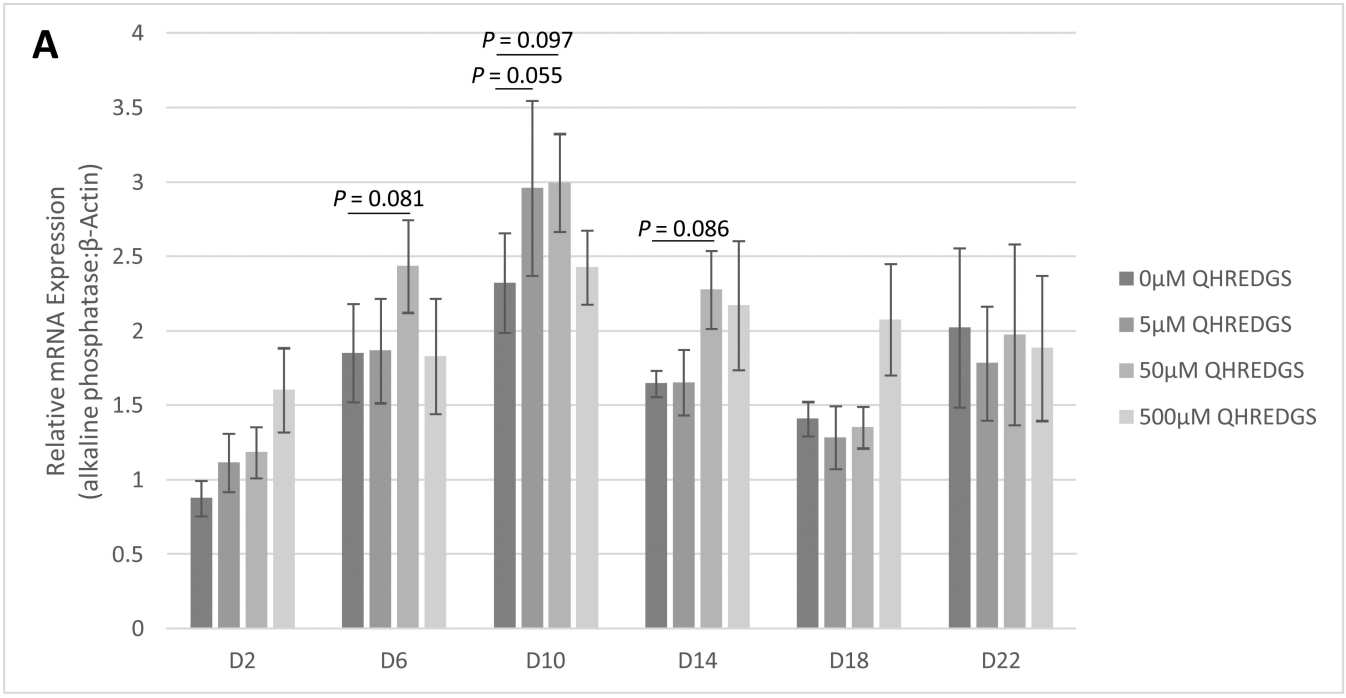

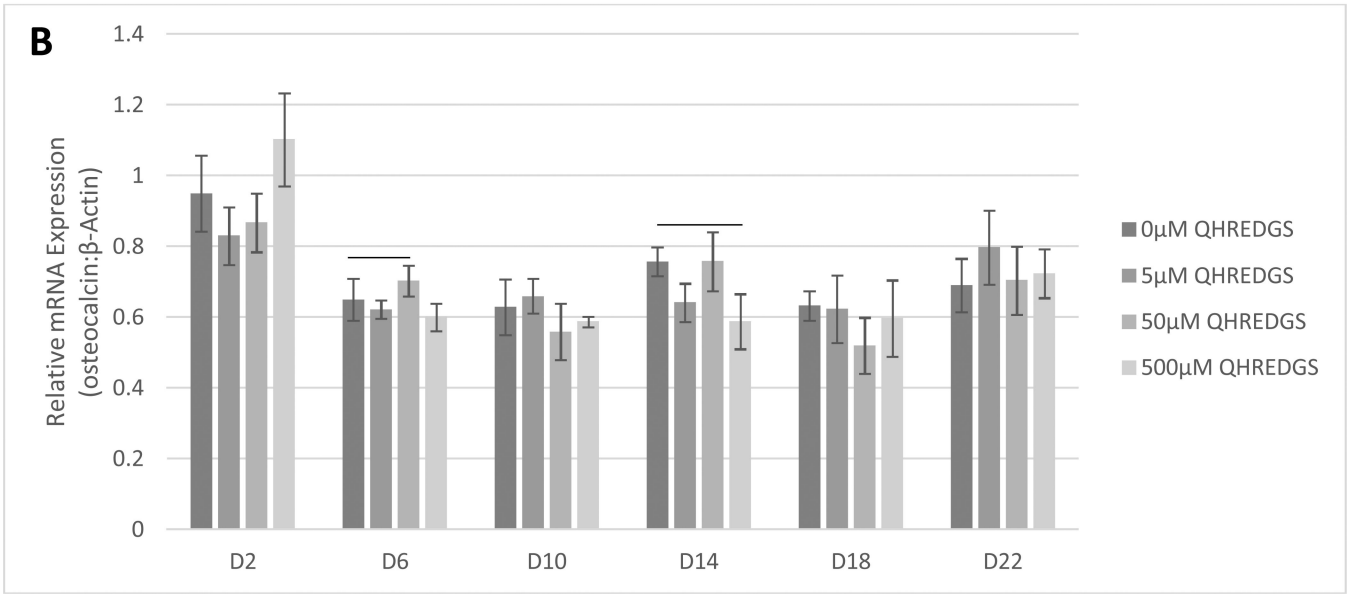

NIH-PA Author Manuscript
NIH-PA Author Manuscript
NIH-PA Author Manuscript

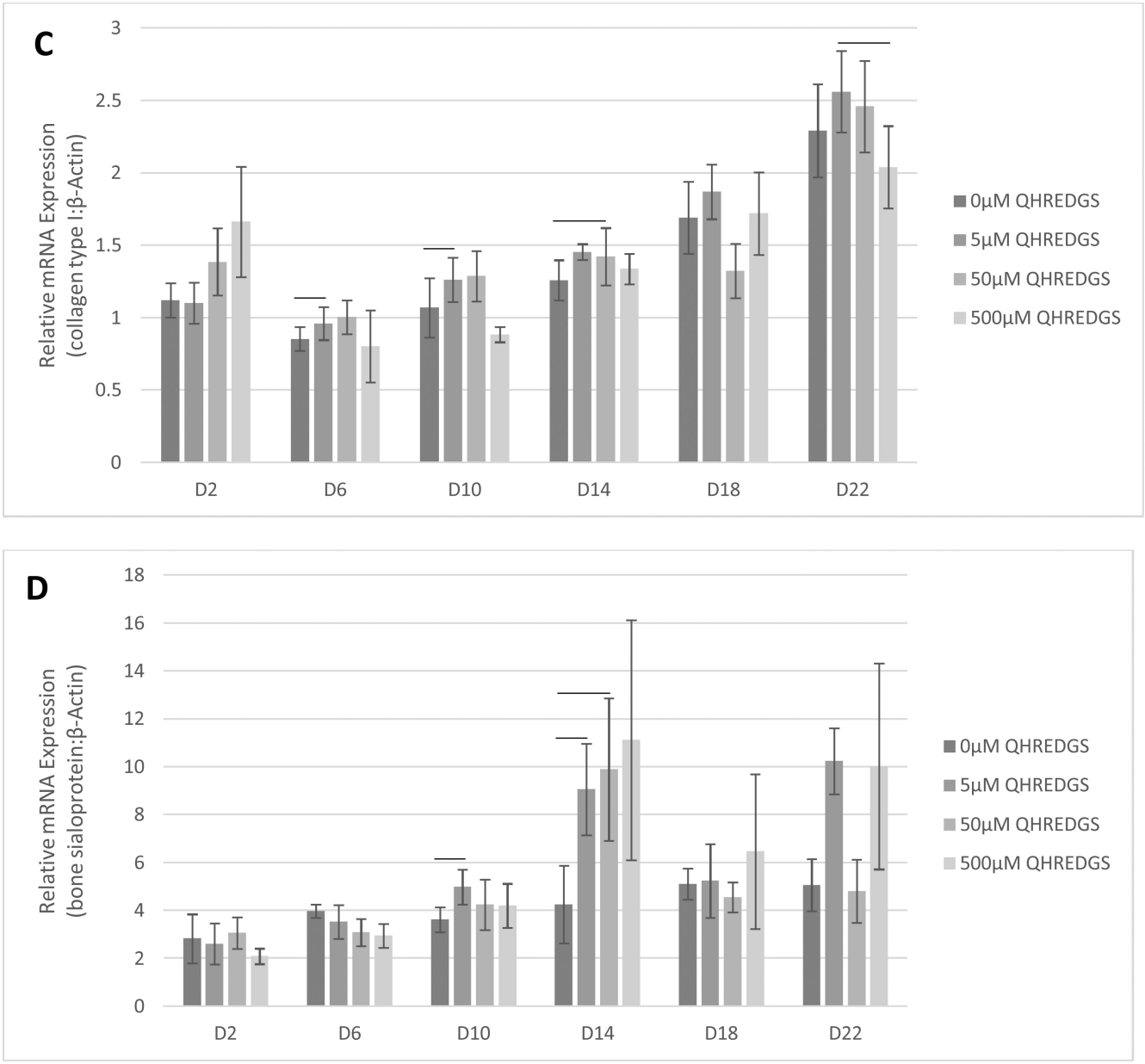

FIGURE 3.

Osteogenic gene expression of osteoblasts grown on tissue culture plastic in the presence or absence of soluble QHREDGS on the indicated day (D): **(A)** alkaline phosphatase, **(B)** osteocalcin, **(C)** type I collagen and **(D)** bone sialoprotein. Gene expression was normalized by dividing by the expression of the housekeeping gene β-actin. Data presented are the mean ± SEM (n=3) and the lines indicate statistical significance ($P < 0.05$, unless noted, n=3).

NIH-PA Author Manuscript

NIH-PA Author Manuscript

NIH-PA Author Manuscript

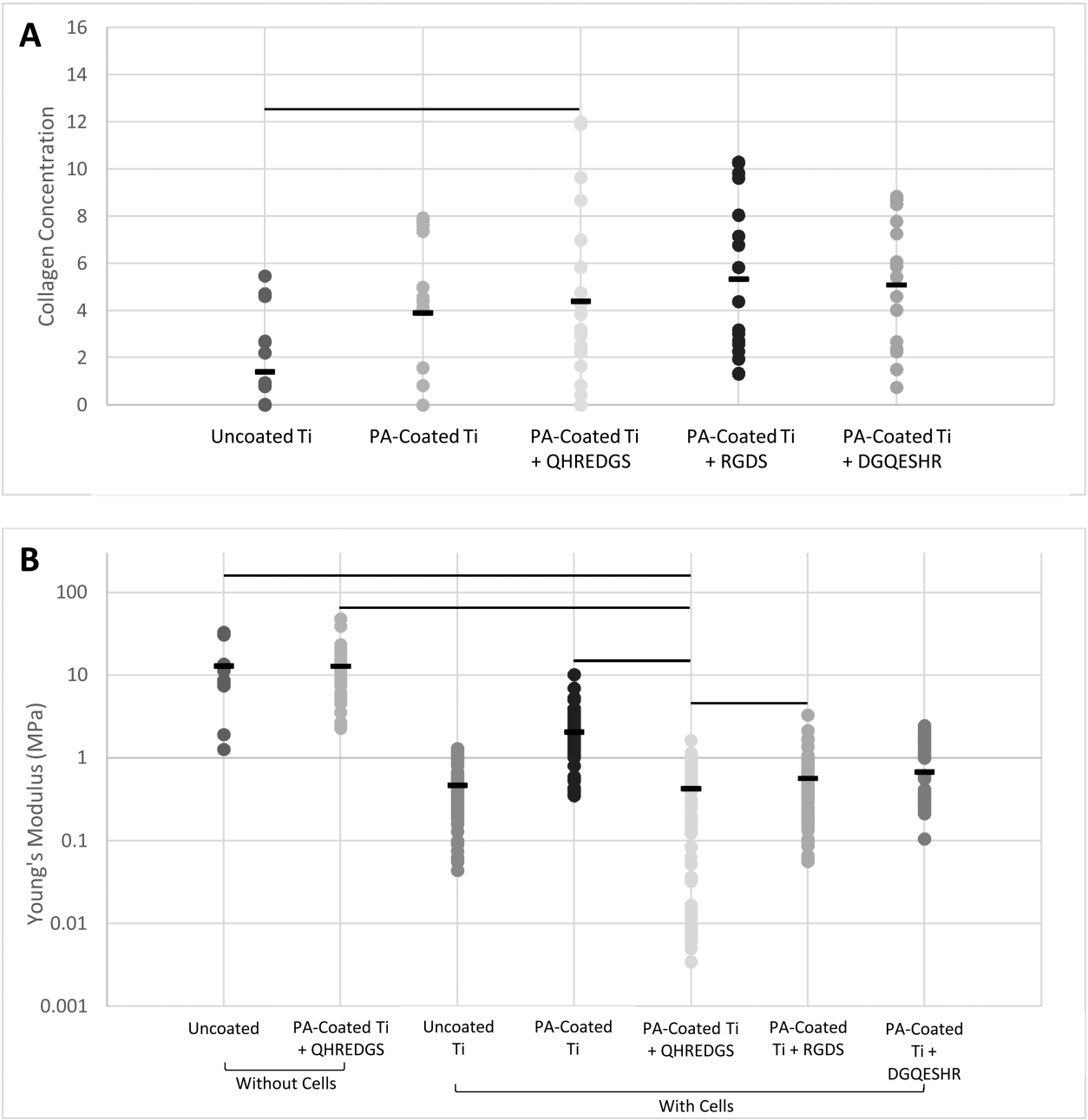

Figure 4.

Bone extracellular matrix production measurements. **(A)** The collagen concentration of the demineralized bone matrix was determined from FTIR spectra (650-4000 cm^{-1}) for osteoblasts grown on Ti plates without the PA-coating (*Uncoated Ti*), PA-coated but without any peptide conjugated (*PA-Coated Ti*), or PA-coated with QHREDGS, RGDS or DGQESHR (scrambled) peptide conjugated. **(B)** The elastic (Young's) modulus of Ti plates with or without peptide immobilized and without any cells seeded on them (*Without Cells*), and of the demineralized bone matrix laid down by the osteoblasts seeded on the various surfaces (*With Cells*) was determined by AFM. The data presented are the individual measurements with the mean denoted by the black dash. The lines indicate statistical

significance ($P < 0.05$; Kruskal-Wallis one-way ANOVA on ranks and Dunn's post-hoc analysis; n=3-7).

NIH-PA Author Manuscript

NIH-PA Author Manuscript

NIH-PA Author Manuscript

NIH-PA Author Manuscript

NIH-PA Author Manuscript

NIH-PA Author Manuscript

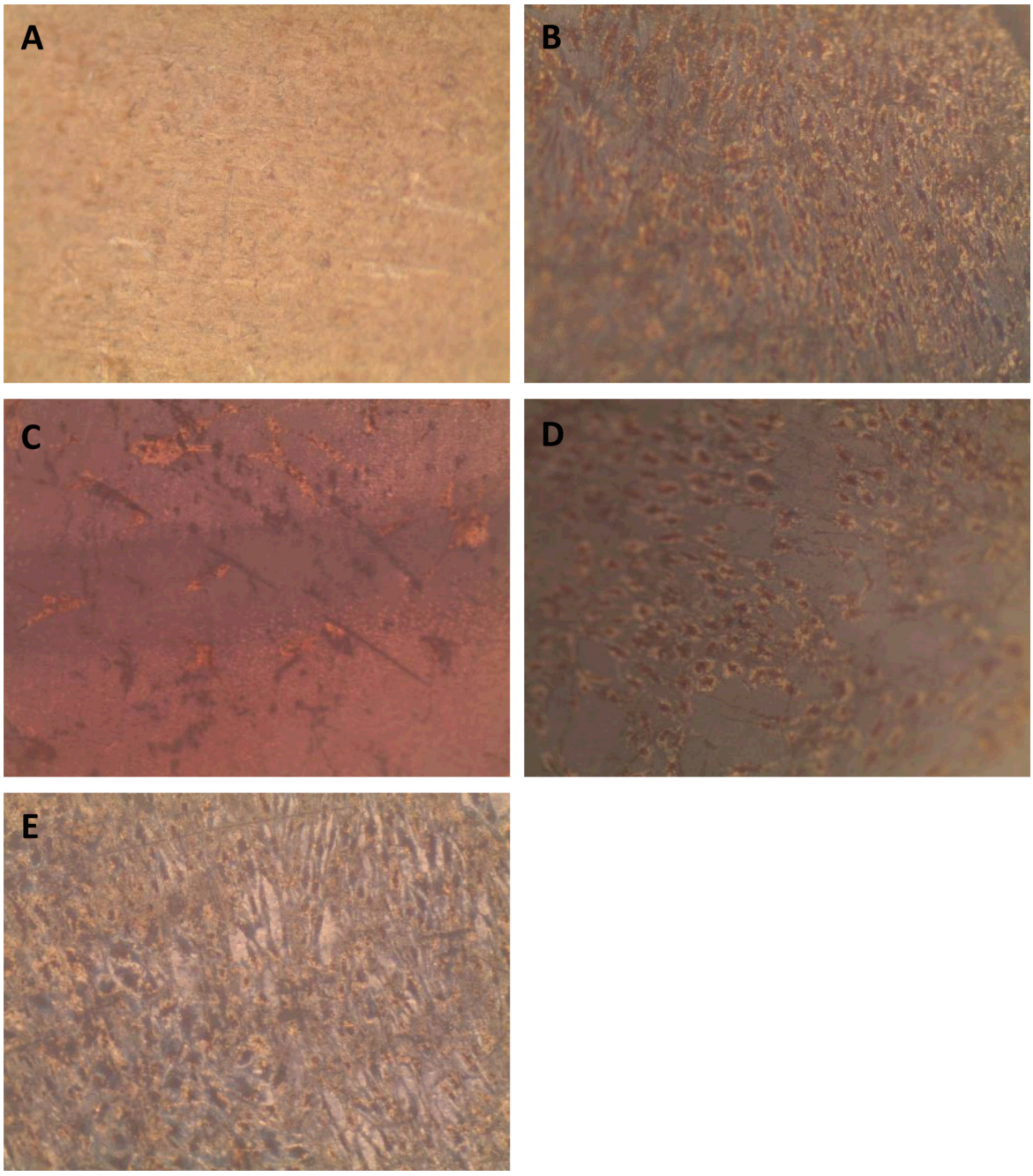

Figure 5.

Representative Alizarin Red S and von Kossa staining images of Ti plates with various coatings seeded with osteoblasts and cultured in osteogenic media for 41 days. **(A)** Ti plates without the PA-coating. **(B)** PA-coated Ti plates without any peptide immobilized. **(C)** PA-coated Ti plates immobilized with QHREDGS peptide. **(D)** PA-coated Ti plates immobilized with RGDS peptide. **(E)** PA-coated Ti plates immobilized with DGQESHR (scrambled) peptide.

NIH-PA Author Manuscript

NIH-PA Author Manuscript

NIH-PA Author Manuscript

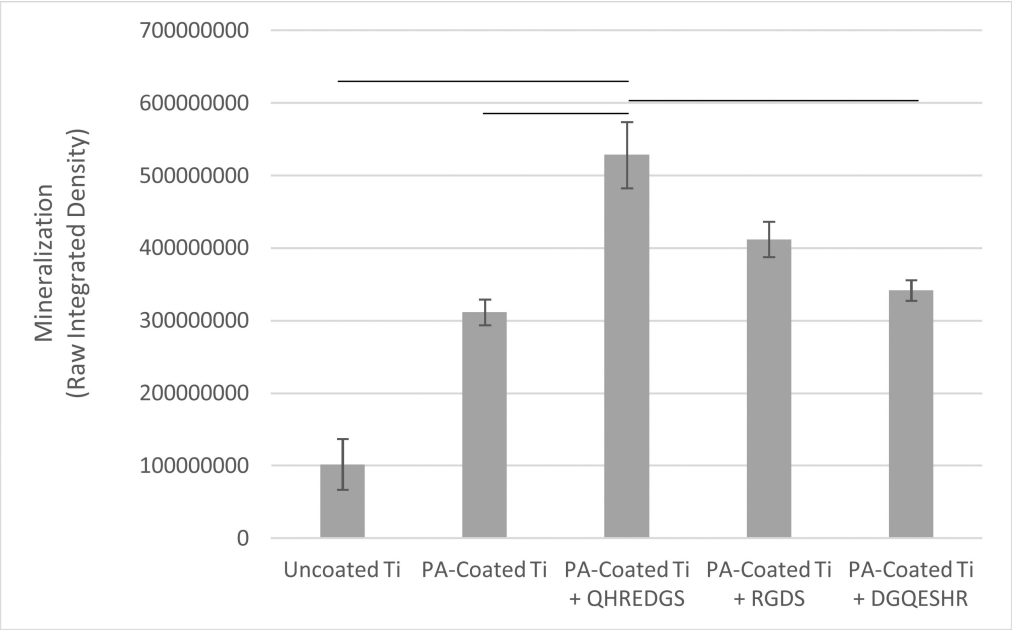

Figure 6.

The amount of Alizarin Red S bound to the surface of Ti plates with various coatings seeded with osteoblasts and cultured in osteogenic media for 41 days, as determined by the sum of the pixel values in the red channel images (raw integrated density). Data presented are the mean ± SEM (n=3) and the lines indicate statistical significance ($P < 0.05$; Kruskal-Wallis one-way ANOVA on ranks and Dunn's post-hoc analysis; n=3).

NIH-PA Author Manuscript

NIH-PA Author Manuscript

NIH-PA Author Manuscript

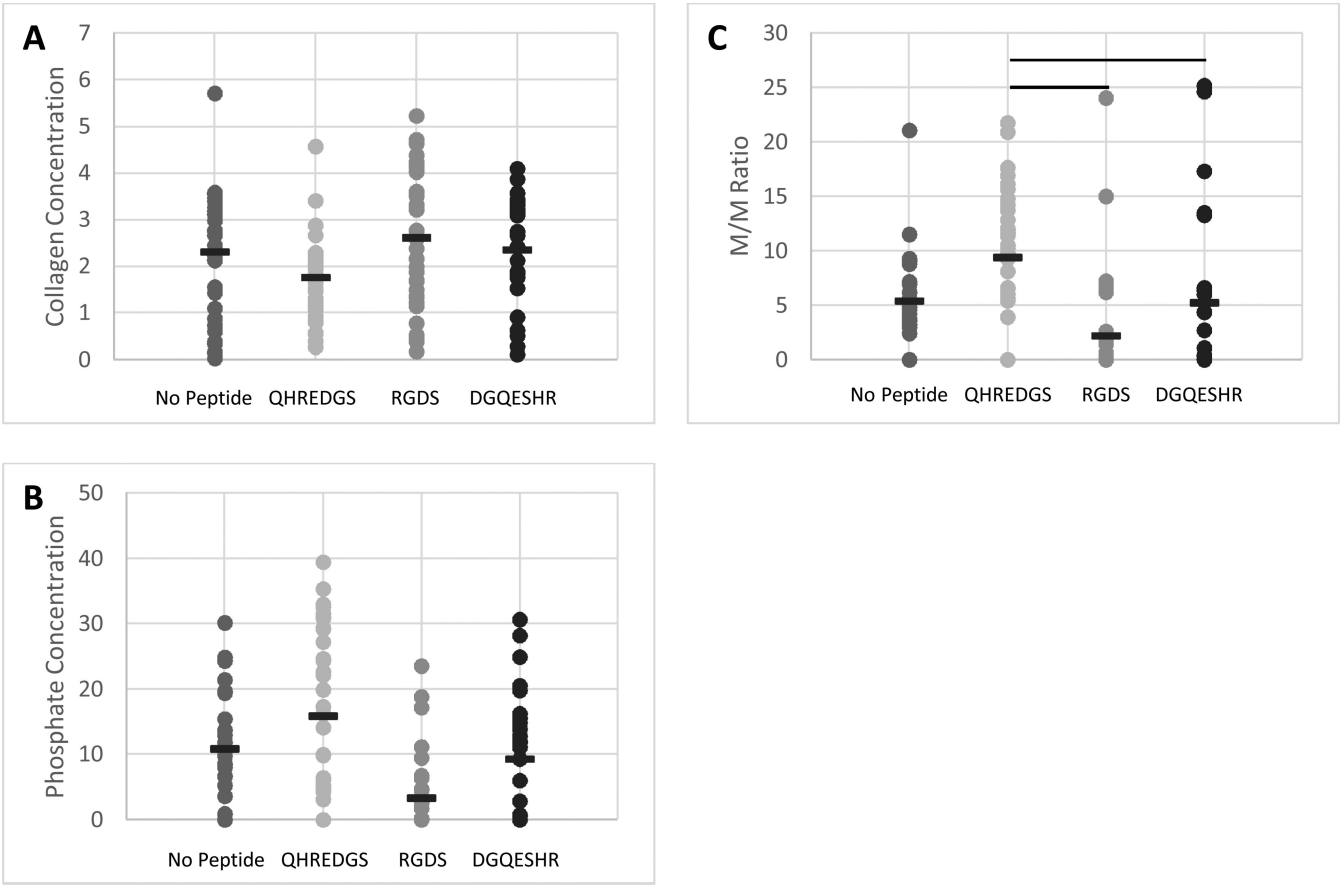

Figure 7.

The composition of bone matrix produced by osteoblasts cultured on PEG-based hydrogels without peptide conjugated (*No Peptide*), or with either the QHREDGS, RGDS or DGQESHR (scrambled) peptide conjugated determined by FTIR. **(A-B)** The collagen (matrix) and phosphate (mineral) concentrations of the bone matrix was determined from the FTIR spectra (650-4000 cm^{-1}). **(C)** The mineral-to-matrix (M/M) ratio was also calculated. The data presented are the individual measurements with the mean denoted by the black dash. The lines indicate statistical significance ($P < 0.05$; Kruskal-Wallis one-way ANOVA on ranks and Dunn's post-hoc analysis; n=4).